energies

MDPI

Article

Selection of an Optimal Frequency for Offshore Wind Farms

Byeonghyeon An, Junsoo Che, Taehun Kim and Taesik Park *

Department of Electrical and Control Engineering, Mokpo National University, Muan 58554, Republic of Korea; shfmql12@mokpo.ac.kr (B.A.); cownstn3177@mokpo.ac.kr (J.C.); kaeu12345@mokpo.ac.kr (T.K.)
* Correspondence: tspark@mokpo.ac.kr

Abstract: Offshore wind power has attracted significant attention due to its high potential, capability for large-scale farms, and high capacity factor. However, it faces high investment costs and issues with subsea power transmission. Conventional high-voltage AC (HVAC) methods are limited by charging current, while high-voltage DC (HVDC) methods suffer from the high cost of power conversion stations. The low-frequency AC (LFAC) method mitigates the charging current through low-frequency operation and can reduce power conversion station costs. This paper aims to identify the economically optimal frequency by comparing the investment costs of LFAC systems at various frequencies. The components of LFAC, including transformers, offshore platforms, and cables, exhibit frequency-dependent characteristics. Lower frequencies result in an increased size and volume of transformers, leading to higher investment costs for offshore platforms. In contrast, cable charging currents and losses are proportional to frequency, causing the total cost to reach a minimum at a specific frequency. To determine the optimal frequency, simulations of investment costs for varying capacities and distances were conducted.

Keywords: low-frequency AC; offshore wind farm; high-voltage AC; high-voltage DC; submarine cable; offshore platforms; optimal frequency

check for updates

Citation: An, B.; Che, J.; Kim, T.; Park, T. Selection of an Optimal Frequency for Offshore Wind Farms. *Energies* **2024**, *17*, 2440. https://doi.org/10.3390/en17102440

Academic Editor: Adrian Ilinca

Received: 19 April 2024
Revised: 10 May 2024
Accepted: 17 May 2024
Published: 20 May 2024

Copyright: © 2024 by the authors. Licensee MDPI, Basel, Switzerland. This article is an open access article distributed under the terms and conditions of the Creative Commons Attribution (CC BY) license (https://creativecommons.org/licenses/by/4.0/).

1. Introduction

To keep pace with the global paradigm shift in the power sector, renewable energy transition policies are being implemented to reduce reliance on coal-fired power generation.

Wind power is considered one of the most important renewable energy resources, and in some countries, wind power accounts for over 20% of their total energy capacity [1]. Offshore wind power, which has potential for large-scale development, low environmental impact, and high capacity (30–50%), has seen increased deployment [2,3]. Europe's offshore wind power capacity reached 25 GW by 2020, with a target set to reach 70 GW by 2030. Additionally, global analyses suggest that 500 GW of offshore wind capacity must be installed by 2030 and a total of 2500 GW is needed by 2050 to curb global warming [4,5]. Such turbines are being constructed farther offshore to maximize wind energy potential. Despite its many advantages, offshore wind power faces challenges such as higher initial investment and operational costs compared to onshore wind power, especially as the distance from the shore increases, posing challenges for long-distance, large-scale power transmission [6,7].

Traditionally, the solution for long-distance alternating current (AC) transmission has been high-voltage alternating current (HVAC). However, offshore wind farms require submarine cables for grid integration with onshore systems. Submarine cables have a higher charging capacity than overhead lines, reducing the maximum transmission capacity is and necessitating compensatory equipment [8]. To address these challenges, high-voltage direct current (HVDC) systems have been proposed as a solution for interconnecting offshore wind farms with the onshore grid [9]. DC transmission, lacking frequency, offers greater flexibility in cable charging capacity and higher transmission capacity compared to AC at the same voltage level. However, the installation of expensive power conversion

equipment on offshore platforms and onshore platforms results in higher initial investment costs. Compared to DC, HVAC has lower platform costs but suffers from a sharp increase in costs with distance due to cable transmission capacity limitations. Therefore, HVAC systems are preferred for short distances, but beyond a certain threshold distance, HVDC systems are advantageous. With the increasing installation of offshore wind power, studies on economic analysis considering power conversion equipment, cable costs, and losses for selecting offshore wind power interconnection platforms are actively underway. The threshold distance for the overall cost of HVAC and HVDC systems is 80 km for submarine cable systems [10–12], while for overhead-line systems, it exceeds 700 km [13,14]. The economic feasibility of distance is not always the determining factor. For example, in overseas offshore wind power projects, while Hornsea [15] and Dogger Bank [16] are in the same region, Hornsea opted for HVAC, whereas Dogger Bank chose HVDC.

LFAC, also known as a fractional frequency transmission system [17–20], is an intermediate system between HVAC and HVDC. Typically, it operates at one-third of the standard frequency of HVAC, which is 20/16.7 Hz, instead of the typical 60/50 Hz. Its lower frequency reduces the impact on the inductive reactance of overhead lines or the capacitive susceptance of cables, resulting in decreased losses and increased transmission capacity. Moreover, it reduces voltage sensitivity to reactive power fluctuations, enhancing voltage stability. LFAC systems were initially applied to overcome joule losses due to the standard frequency in railway systems with increasing distances in countries like Germany, Austria, and Switzerland. They offer improvements in long-distance and submarine power transmission, making them subject to extensive research. Notably, by leveraging the benefits of offshore wind power, research on LFAC systems for interconnecting offshore wind farms addresses issues such as the charging capacity problem of submarine cables in HVAC and the high investment cost of HVDC as installation locations move farther offshore. Figure 1 illustrates the interconnection configuration of offshore wind farms achieved using the aforementioned methods.

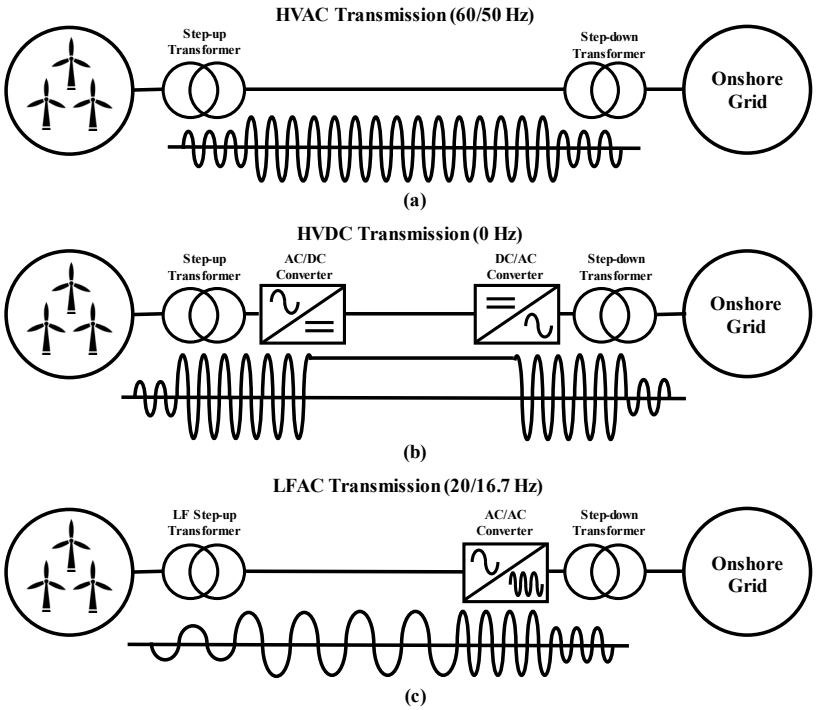

Figure 1. Structure of (**a**) HVAC, (**b**) HVDC, and (**c**) LFAC connection systems.

Evidently, LFAC systems, unlike HVDC, have AC/AC converters installed on only one side, resulting in relatively lower platform costs [21]. Compared to HVAC, LFAC systems have lower losses and higher transmission capacity, leading to lower cable costs.

With these characteristics, the threshold distance for LFAC falls between HVAC and HVDC. Olsen [22] and Hytten [23] analyzed the economic feasibility of offshore wind farm interconnection methods across various distance ranges and suggested that HVAC is economical for distances up to approximately 100 km, LFAC for distances between 100 and 200 km, and HVDC for distances exceeding 200 km. Additionally, Xiang [24] divided the costs of interconnection methods into the terminal cost and route cost and evaluated their economic feasibility by categorizing them into the capital cost and power loss cost to determine cost-efficient distance ranges.

Several studies have verified the economic feasibility of offshore wind farm-interconnecting LFAC systems based on distance. However, in most of these studies, the conventional frequency, 20/16.7 Hz, which is one-third of the standard frequency 60/50 Hz, has been set as the LFAC frequency. Economic analyses of LFAC systems with non-standard frequencies have rarely been conducted. Moreover, frequency variations can impact investment costs related to transformers, offshore platforms, and submarine cables. According to the "2021 Cost of Wind Energy Review" of the National Renewable Energy Laboratory [25], the Levelized Cost of Energy ratio of substructure and foundation construction and electrical infrastructure for offshore wind power has reached 20.6%, indicating a significant portion of lifecycle costs alongside turbine (22.5%) and maintenance (24%) expenses. This paper aims to identify the most economically optimal frequency for LFAC systems by comparing total system costs under non-standard frequency operations. To achieve this, this study calculates the investment costs of frequency-dependent components and transmission costs from cables. In the case of transformers, lower frequencies lead to increased volume and weight to maintain constant flux, while the costs of offshore platforms are determined based on the weight of the equipment installed on top. As a result, the costs of transformers and offshore platforms have an inverse relationship with frequency. As previously mentioned, the primary constraint in subsea power transmission is the capacity limitation due to the charging current. The charging current decreases with lower frequency, increasing transmission capacity. Therefore, assuming the same capacity, the number of cables required decreases as frequency decreases, leading to transmission costs that are inversely proportional to frequency. Considering these characteristics of different components, there is a specific frequency at which the total cost of the LFAC system is minimized. This varies with capacity and distance, so simulations were conducted under different conditions to find the optimal frequency.

2. Frequency Dependence Analysis of LFAC Components for Connection to Offshore Wind Farms

The components of an offshore wind farm-interconnecting LFAC system can be broadly categorized as step-up low-frequency transformers, offshore platforms, submarine cables, and frequency conversion devices. Among these, the frequency conversion device, which allows the conversion of standard frequencies to low frequencies or vice versa, is one of the most critical elements of an LFAC system.

A rotary frequency converter, consisting of two electrical machines widely used in railways, is the most commonly employed frequency conversion device in LFAC systems [26,27]. However, such a converter exhibits poor mechanical-power transmission efficiency and is characterized by a fixed input–output frequency ratio, which is determined by the poles of the machine. To address these issues, back-to-back (BTB) converters based on power electronics technology have been proposed [21,28,29]. Voltage-type BTB converters facilitate frequency conversion and power control; however, they use expensive power electronic components and generate harmonics, which increase their costs. Therefore, recently, several studies on modular multilevel matrix converters, which are beneficial for AC/AC conversion, have been reported [30–32].

Analyzing LFAC systems requires frequency conversion devices, and considering integration with offshore wind farms, these devices should be installed at the connection point with the existing grid. Assuming the power conversion equipment operates reliably

at frequencies above 10 Hz, the investment cost of frequency conversion devices generally varies based on the rated voltage and capacity. Consequently, it can be assumed that investment costs do not change with frequency variation. Taking these characteristics into account, this study focuses its analysis on frequency-dependent elements such as transformers, offshore platforms, and subsea cables.

2.1. Design of Power Transformers

Variations in frequency can significantly impact the design of power transformers. The magnetic flux of a transformer can be expressed as follows:

$$E = 4.44 f N B_m A_{core}, \tag{1}$$

where f represents the rated frequency, N is the number of turns, B_m denotes the maximum magnetic flux density, and A_{core} represents the core area. If the frequency decreases, then the number of turns, maximum magnetic flux density, and core area must increase to maintain the same power. Therefore, in such cases, large and wide low-frequency transformers are required to maintain the same power level. These changes in the number of turns and core area imply an increase in the use of copper and iron in the transformer, and therefore its weight and price.

The cost of transformers designed for standard frequencies can be calculated based on transformer rated power using the following formula [33]:

$$\begin{array}{c} LV/MV : C_{tr50} = -0.162 + 0.139 \times S_{tr}^{0.447}, \\ MV/HV : C_{tr50} = 0.045 \times S_{tr}^{0.751}, \end{array} \tag{2}$$

where C_{tr50} represents the cost of a 50 Hz transformer (in M$), and S_{tr} denotes the rated power of the transformer (in MVA).

As mentioned earlier, the size, weight, and cost of low-frequency transformers are expected to increase compared to transformers designed for standard frequencies. Assuming that the maximum magnetic flux density is kept constant for the regular operation of the transformer, we can define the changes in volume and overall area of the core and winding due to frequency variation through first-order approximation as follows [34].

$$\begin{array}{c} V_{core}, V_{winding} \propto \frac{1}{f_r}, \\ A_{enc} \propto \frac{1}{\sqrt[3]{f_r^2}}, \end{array} \tag{3}$$

where V_{core} represents the volume of the core, $V_{winding}$ denotes the volume of the winding, A_{enc} indicates the overall area, and f_r represents the non-standard frequency ratio (standard frequency/nominal frequency). Therefore, the amount of raw material required for the transformer varies according to the nominal frequency. Considering the percentage of transformer cost presented in Table 1, the transformer cost according to frequency can be calculated as follows [34]:

$$C_{tr} = \frac{0.325 f_r + 0.22 f_r + 0.164 \sqrt[3]{f_r^2}}{0.325 + 0.22 + 0.164} \times C_{tr50}. \tag{4}$$

Figure 2 illustrates the cost variation for a 100 MVA power transformer from 10 to 120 Hz. As the frequency increases, the transformer cost decreases, with approximately a ninefold difference in cost between 10 and 120 Hz.

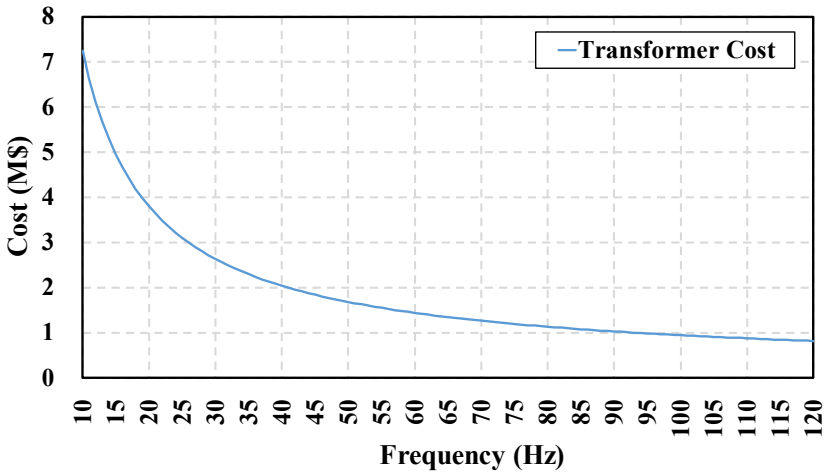

Figure 2. Power transformer cost versus frequency.

Table 1. Percentages of overall costs of materials used to manufacture a transformer [35].

Transformer Material	Cost (%)
Magnetic steel	32.5 ± 5.5
Windings	22.0 ± 6.0
Insulation	14.1 ± 5.5
Carbon steel	16.4 ± 8.5
Fabricated parts	15.0 ± 9.0

2.2. Offshore Platforms

Offshore wind power requires offshore platforms, such as offshore substations, to transmit the generated power to the onshore grid. Owing to their construction in the sea, the selection of substructures is crucial and can be divided into fixed and floating types depending on the water depth. Fixed structures are used for depths below 60 m, while floating structures are applied for depths exceeding 60 m. Approximately 99.8% of the offshore wind turbines installed before 2022 worldwide are fixed structures, indicating that floating structures are still in the early stages of development. Even within fixed structures, variations due to water depth and ground conditions occur; such variable structures are categorized into gravity-based, monopile, jacket, and tripod types, whose characteristics are outlined in Table 2 [36].

Table 2. Comparison of fixed substructure types of offshore wind turbines.

	Gravity	Monopile	Jacket	Tripod
Depth of water [m]	~30	~30	10–60	20–60
Advantages	Simplicity of structure Ease of installation High safety	Lightweight/simple structure Ease of installation	Lightweight High strength	Lightweight High safety
Disadvantages	Constraints on the ground Heavy weight Long construction duration	Constraints on the ground Induces terrain changes	Constraints of weather conditions	Constraints on the ground Fixed offshore installation platform is required

Currently, over 70% of fixed structures are of the monopile type, while jacket-type structures are commonly used in relatively deep waters (30–60 m). However, the average water depth for offshore wind farms is approximately 33 m, and there is a trend toward venturing into deeper seas to maximize the potential of offshore wind energy. Considering this trend, we assume a water depth of 40 m and select jacket-type substructures. Figure 3 illustrates the critical elements of a jacket-type structure [37].

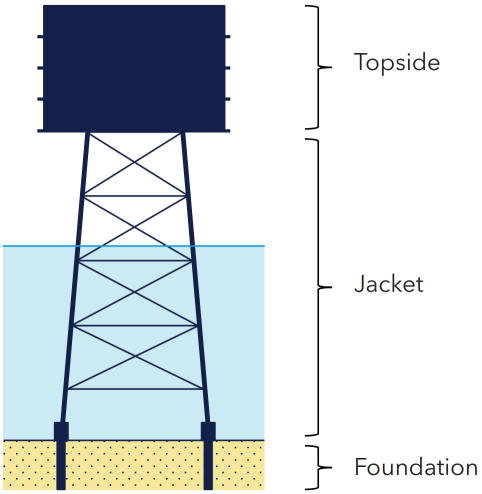

Figure 3. Main elements of an offshore jacket platform.

The factors influencing the substructure of offshore platforms are water depth and weight, and the cost for each essential element can be expressed as follows [37]:

$$C_{topside} = topside\ mass\ [\text{ton}] \times 0.00795, \tag{5}$$

$$C_{jacket} = jacket\ mass\ [\text{ton}] \times 0.00371, \tag{6}$$

$$jacket\ mass\ [\text{ton}] = water\ depth\ [\text{m}] \times 1.7 \times topside\ mass\ [\text{ton}]^{0.4557}, \tag{7}$$

$$C_{pile/foundation} = ((0.0235 \times (jacket\ mass\ [\text{ton}] + topside\ mass\ [\text{ton}]) + 534) \times 0.00159, \tag{8}$$

where $C_{topside}$, C_{jacket}, and $C_{pile/foundation}$ represent the cost (M$) of the topside, jacket, and foundation, respectively.

In an offshore wind power-generation platform, the weight of the topside can vary per frequency, depending on the transformers and shunt reactors used for reactive power compensation. The weight distribution of transformers is shown in Table 3, primarily consisting of electrical steel sheets, steel, copper, and insulating oil. Applying this to the volume change in transformers according to frequency, the weight of a transformer per frequency can be represented as follows:

$$W_{tr} = \left(0.56 f_r + 0.38 \sqrt[3]{f_r^2} + 0.06\right) \times W_{tr50}, \tag{9}$$

where W_{tr} and W_{tr50} represent the weight of a non-standard frequency transformer and 50 Hz frequency transformer, respectively. Typically, the weight of a transformer with the same frequency, voltage, and capacity is proportional to approximately 0.7 to 0.8 times the capacity. Additionally, when the capacity, frequency, and voltage are the same, the weight of a single-phase transformer is approximately 80% of the weight of a three-phase transformer. In this study, we assumed the feasibility of transporting transformers; therefore, the weight was calculated based on a three-phase batch transformer. The weight of a transformer varies depending on the structure, manufacturer, and materials used, so a general transformer is assumed (132 kV/20 MVA/40 tons, 220 kV/150 MVA/200 tons).

Table 3. Percentages of the weights of raw materials used in a power transformer.

Transformer Raw Material	Weight (%)
Electrical steel	40
Steel	19
Transformer oil	19
Copper	16
Other	6

The structure of the shunt reactor for power factor correction is similar to that of a power transformer. Therefore, the weight of a shunt reactor is typically calculated as two-thirds of the weight of a transformer with the same capacity. Owing to their similar structures, we assume that the weight and cost changes due to frequency are the same for shunt reactors and transformers, and thus, the weight of a shunt reactor is estimated to be two-thirds of the weight of a transformer with the same capacity.

The amount of steel required for the topside structure of an offshore platform should be assumed to be equal to the weight of the installed equipment, as it needs to support the weight of the installed systems. Therefore, the topside mass can be calculated as twice the weight of the equipment. Figure 4 illustrates the variation in the weight of the topside structure with the application of a 100 MVA power transformer. As the frequency increases, the weight decreases, and an approximately 6.5-fold difference in weight between 10 and 120 Hz is evident.

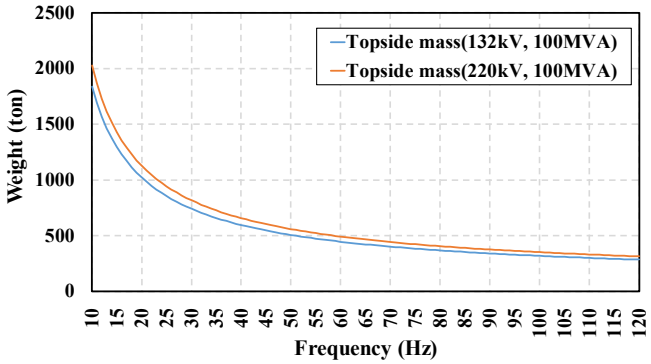

Figure 4. Topside mass versus frequency.

Based on this, the cost of the offshore platform substructure by frequency is calculated as shown in Figure 5. Because the basic construction costs are not significantly influenced by frequency, an approximately threefold difference is observed in the substructure cost between 10 and 120 Hz.

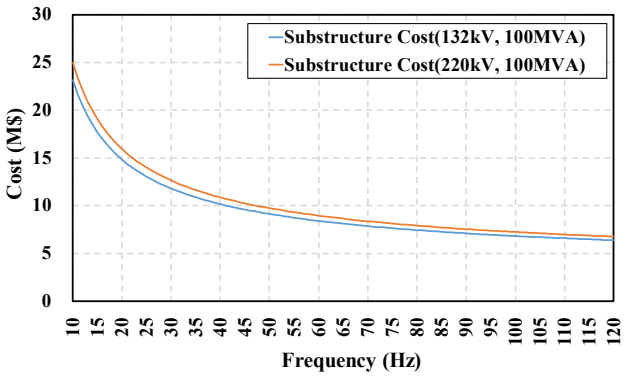

Figure 5. Substructure cost versus frequency.

2.3. Submarine Cable

2.3.1. Transmission Capacity of the Cable

In AC systems, a charging current occurs, which interferes with power transmission through the cables. The charging current is generated through the shunt capacitance of the cable and increases with the cable length and voltage levels, playing a crucial role in cable selection. The charging current of the cable can be expressed as follows:

$$I_c = \frac{E\omega CL}{\sqrt{3} \times 10^3}, \tag{10}$$

where I_c represents the charging current (A), E is the rated voltage (kV), ω is the angular frequency of the voltage, C is the capacitance per unit length (μF/km), and L is the cable length (km). The reactive power generated in the cable due to this charging current is defined as follows:

$$Q_c = I_c E \times 10^{-3}, \tag{11}$$

where Q_c represents the reactive power (Mvar). Therefore, the effective power transmission capacity of the cable can be expressed as follows:

$$P = \sqrt{S^2 - {Q_c}^2}, \tag{12}$$

where P represents the effective power at the receiving end (MW), and S represents the generating capacity (MVA). Equations (10)–(12) show that the effective power transmission capacity of the cable increases as the frequency decreases. Figure 6 illustrates the effective power transmission capacity of 132 and 220 kV 1000 mm^2 cables according to frequency and length. As the rated voltage increases, the transmission capacity increases, but the reactive power also increases, resulting in shorter transmission lengths.

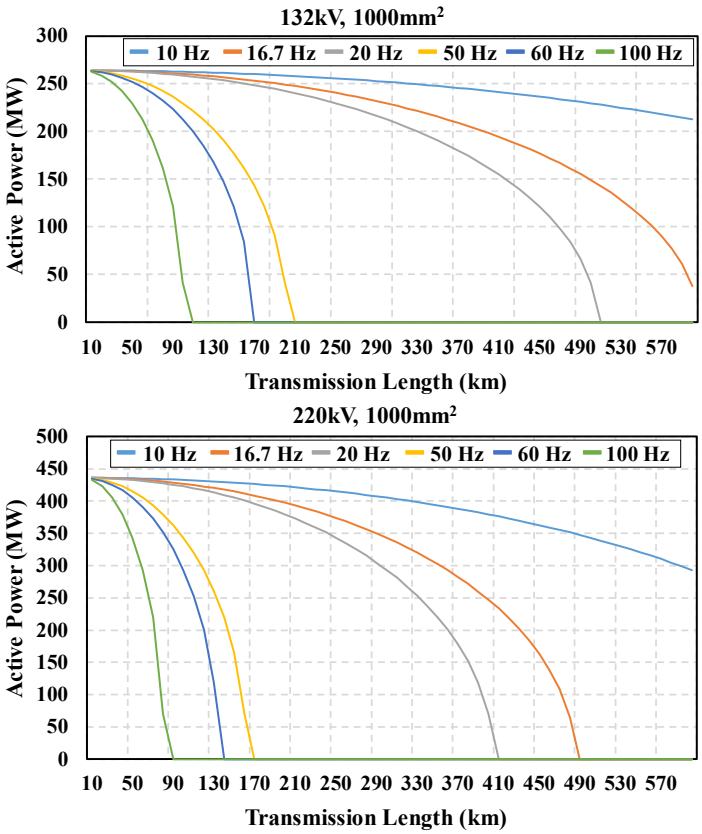

Figure 6. Transmission capability curves at different frequencies.

2.3.2. Transmission Capacity of the Cable

As shown in Figure 6, even with the same cable specifications, increasing the frequency results in a change in the charging current, leading to a decrease in the current delivered to the load. Therefore, for designing cables suitable for transmission distances, the operating frequency, voltage, capacity, cable capacitance, and other factors need to be considered. As evident from Equation (10), as the transmission distance increases, the charging current increases, and the length at which the charging current equals the supply current is defined as the critical transmission distance of a cable, which is defined as follows:

$$L_c = \frac{\sqrt{3} I_s}{\omega C E} \times 10^3, \tag{13}$$

where L_c represents the critical distance of the cable (km), and I_s denotes the supply current (A). Figure 7 illustrates the critical distance at the rated capacity of the cable.

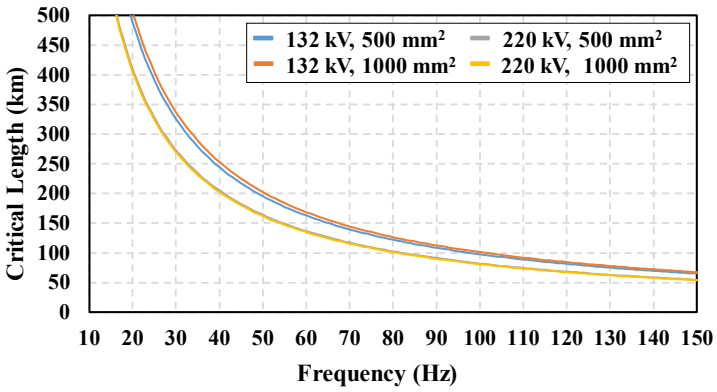

Figure 7. Critical length of cables vs. frequency.

At the rated capacity of the cable, as the frequency increases, the critical transmission length sharply decreases. As mentioned earlier, higher voltages result in larger charging currents, leading to shorter critical transmission distances. Moreover, with larger specifications, the capacitance per unit length of the cable increases, further shortening the critical length.

2.3.3. Number of Cables

Based on the findings from Figure 6, we assessed the effective power transmission capacity of the cable. As the frequency increases, the transmission capacity decreases, implying a potential need for an increased number of cables to deliver power from offshore wind farms. The required number of cables based on the rated capacity of the cable can be defined as follows:

$$N_c = \frac{S}{P}, \tag{14}$$

where N_c represents the number of cables. Figure 8 illustrates the number of cables required at different frequencies based on the cable specifications. These results were determined by assuming a distance of 120 km, a rated voltage of 220 kV, and a capacity of 500 MVA. Because the number of cables must always be an integer (fractions are not possible), the solid lines in Figure 8 represent the calculated number of cables, while the dashed lines represent the actual number of cables.

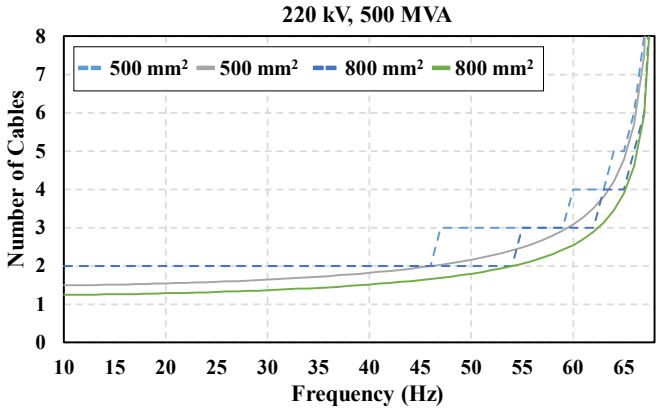

Figure 8. Number of cables required for different operating frequencies (fractional and integer).

2.3.4. Compensation of Reactive Power

Generally, shunt reactors are applied to compensate for the reactive power generated by the cables in offshore wind power systems. Typically, reactive power compensation is considered from the point where the cable utilization is 85%, which corresponds to 15% of the maximum power [38]. The amount of reactive power generated at this point is given by Equation (10). In this study, the cost of reactive power compensation was assumed to be 0.031 (M$/Mvar) [24].

2.3.5. Cable Loss

The losses in the cable are primarily due to the heat generated by the resistance within the cable during current flow. These losses are proportional to the square of the current flowing through the cable, its resistance, and its length, and can be expressed as follows:

$$P_{loss} = \left(\frac{I_s}{N_c}\right)^2 RLN_c, \tag{15}$$

where P_{loss} represents the cable loss, and R denotes the resistance per unit length of the cable. Additionally, as the frequency decreases, the skin depth increases, resulting in a decrease in the resistance of the cable [21]. However, previous studies show that when the frequency is increased from 0 to 60 Hz, the resistance increases by approximately 0.2%, and the inductance increases by ~0.1% [39]. However, under steady-state conditions, the changes in skin effect due to frequency are negligible and can be ignored.

The losses are quantified by considering the offshore wind power selling price, utilization rate, and project duration as follows:

$$C_{loss} = P_{loss}\rho_{off}C_{off}D_{off}\left(\frac{I_s}{N_c}\right)^2 RLN_c, \tag{16}$$

where C_{loss} represents the cost of losses, ρ_{off} is the offshore wind power utilization rate (0.22), D_{off} is the offshore wind power project duration (20 years), and C_{off} is the offshore wind power selling price (0.00025 M$/MWh).

2.3.6. Cable Cost

Cables vary in terms of capacitance, rated current, and cost depending on the rated voltage and specifications. Additionally, cable length and quantity are determined by distance and capacity. Therefore, cables play a crucial role in the selection of optimal frequencies for offshore wind power-generation sites. The cable prices referenced in this paper are shown in Table 4. Figure 9 illustrates the variation in cable costs according to distance and capacity for a 132 kV, 630 mm^2 cable specification. As the frequency increases, the transmission capacity of the table decreases, leading to an increase in the number of

cables and, consequently, the investment cost. Evidently, investment costs increase with increasing capacity and transmission distance.

Table 4. Parameters of cables used in LFAC system.

Nominal Voltage (kV)	Cable Size (mm^2)	Resistance (mΩ/km)	Capacitance (nF/km)	Nominal Current (A)	Cable Cost (M$/km)
132	500	32.6	192	899	0.787
	630	26.2	209	995	0.849
	800	21.5	217	1080	0.986
	1000	18.2	238	1154	1.066
220	500	32.4	136	890	1.011
	630	25.9	151	982	1.054
	800	21.1	163	1069	1.209
	1000	17.9	177	1145	1.240

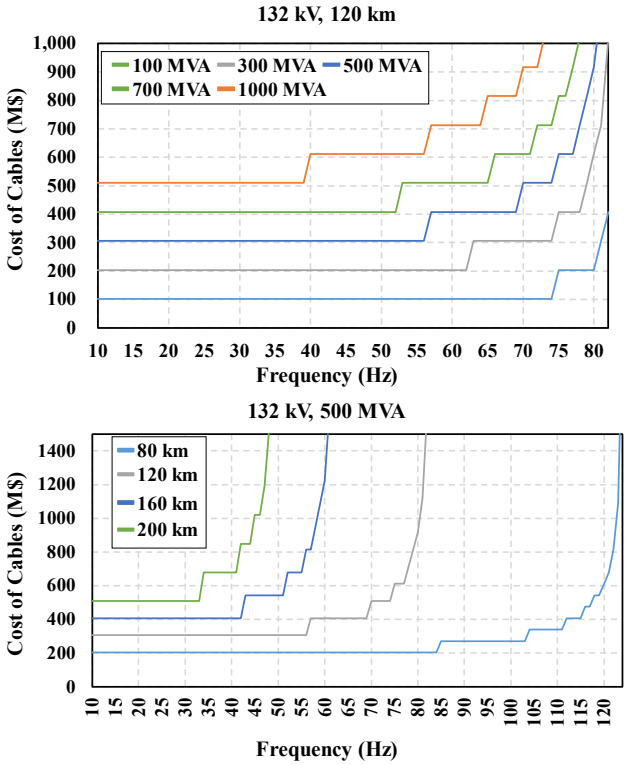

Figure 9. Cost of cables under different operating conditions (630 mm^2).

3. Optimal Frequency Simulation of An Offshore Wind Farm-Connected LFAC System

In this study, simulations were conducted to determine the optimal frequency based on equipment that varies with frequency in the LFAC system-interconnecting offshore wind power-generation sites. The simulation aimed to identify the frequency at which the investment and operational costs are minimized. Previous studies evaluating the economic viability of LFAC systems indicated their viability at distances ranging from 80 to 200 km. Therefore, in this study, the simulation for selecting the optimal frequency was conducted for distances of 80, 120, 160, and 200 km. Additionally, considering the decrease in cable transmission threshold distance with increasing voltage level, rated voltages of 132 and 220 kV were selected, and the capacities were increased from 100 to 1000 MVA to observe variations in the optimal frequency.

3.1. Selection of Optimal Frequency and Cable

Previously, transformers and offshore platforms exhibited a characteristic where frequency and cost are inversely proportional. In contrast, the cable and reactive power compensation costs increase with frequency owing to the proportional charging current, leading to increased expenses with increasing frequency. Moreover, due to the limitation on power transmission capacity, an increase in cables leads to increased losses. Therefore, the total cost of an offshore wind farm-interconnecting LFAC system reaches a minimum at a specific frequency. Figures 10 and 11 illustrate the total investment costs and optimal frequency points by distance at a rated voltage of 132 kV, and Figures 12 and 13 present the simulation results obtained for a rated voltage of 220 kV.

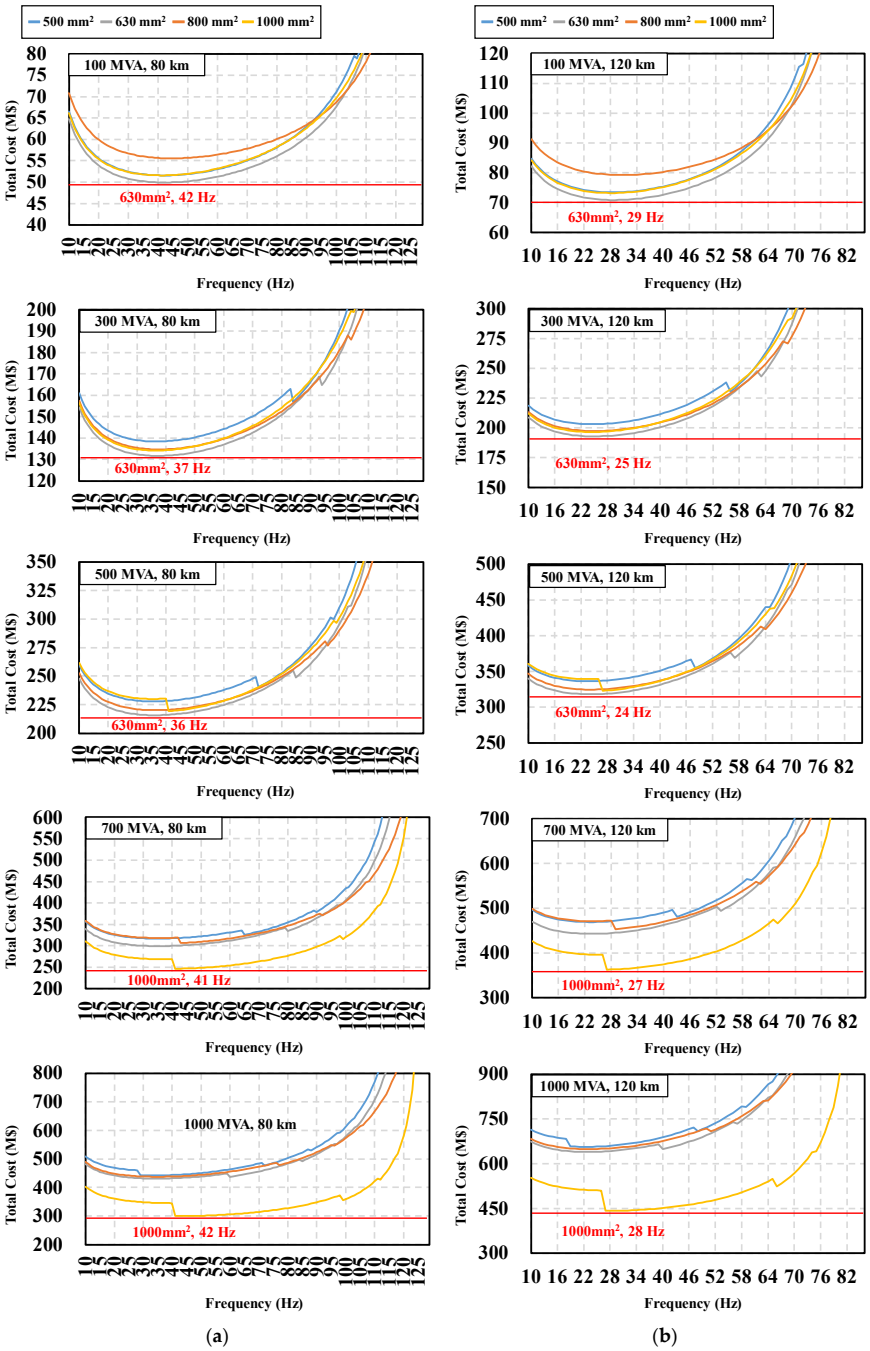

Figure 10. Total cost versus operating frequency at 132 kV: (**a**) 80 km; (**b**) 120 km.

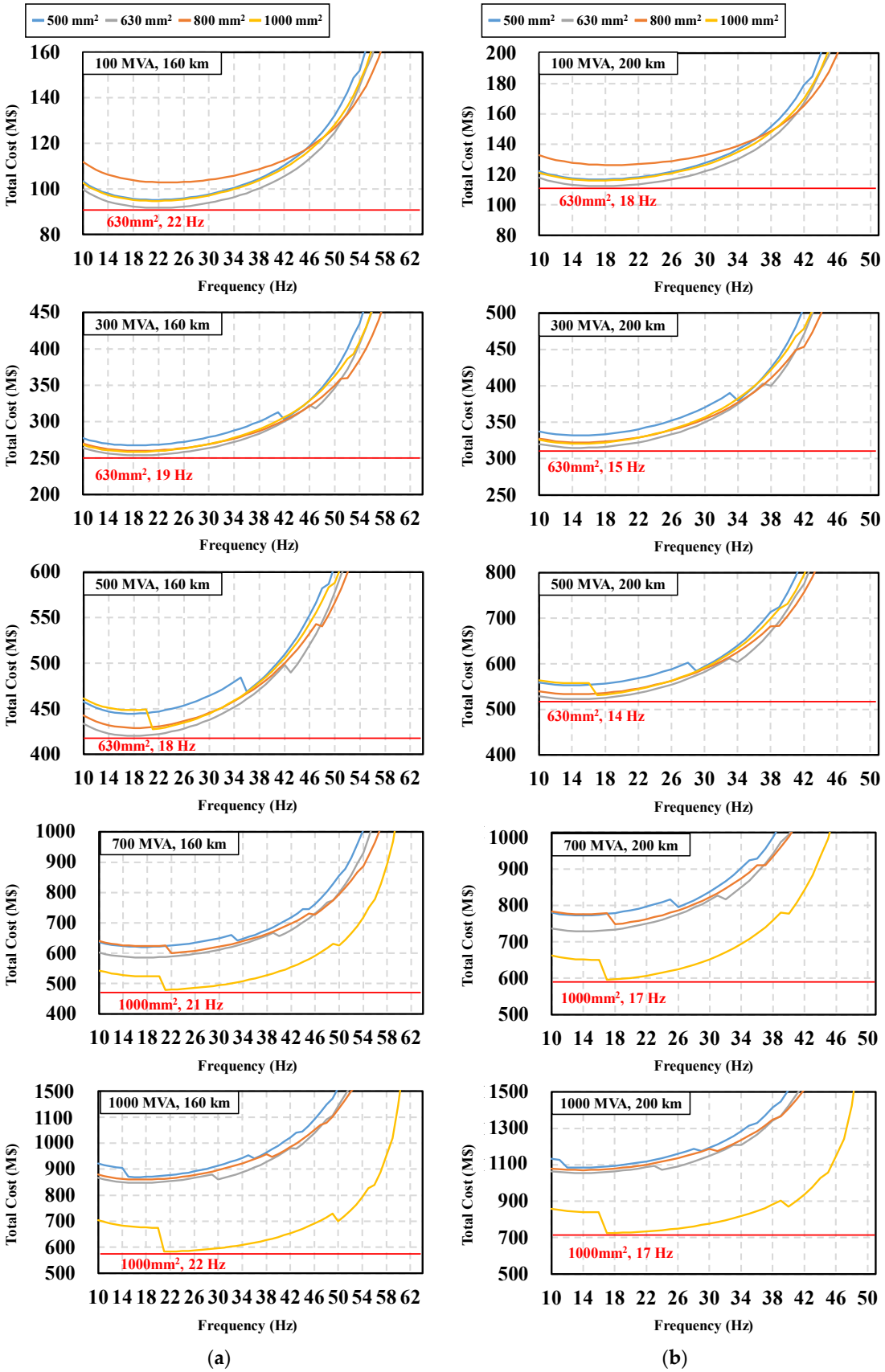

Figure 11. Total cost versus operating frequency at 132 kV: (**a**) 160 km; (**b**) 220 km.

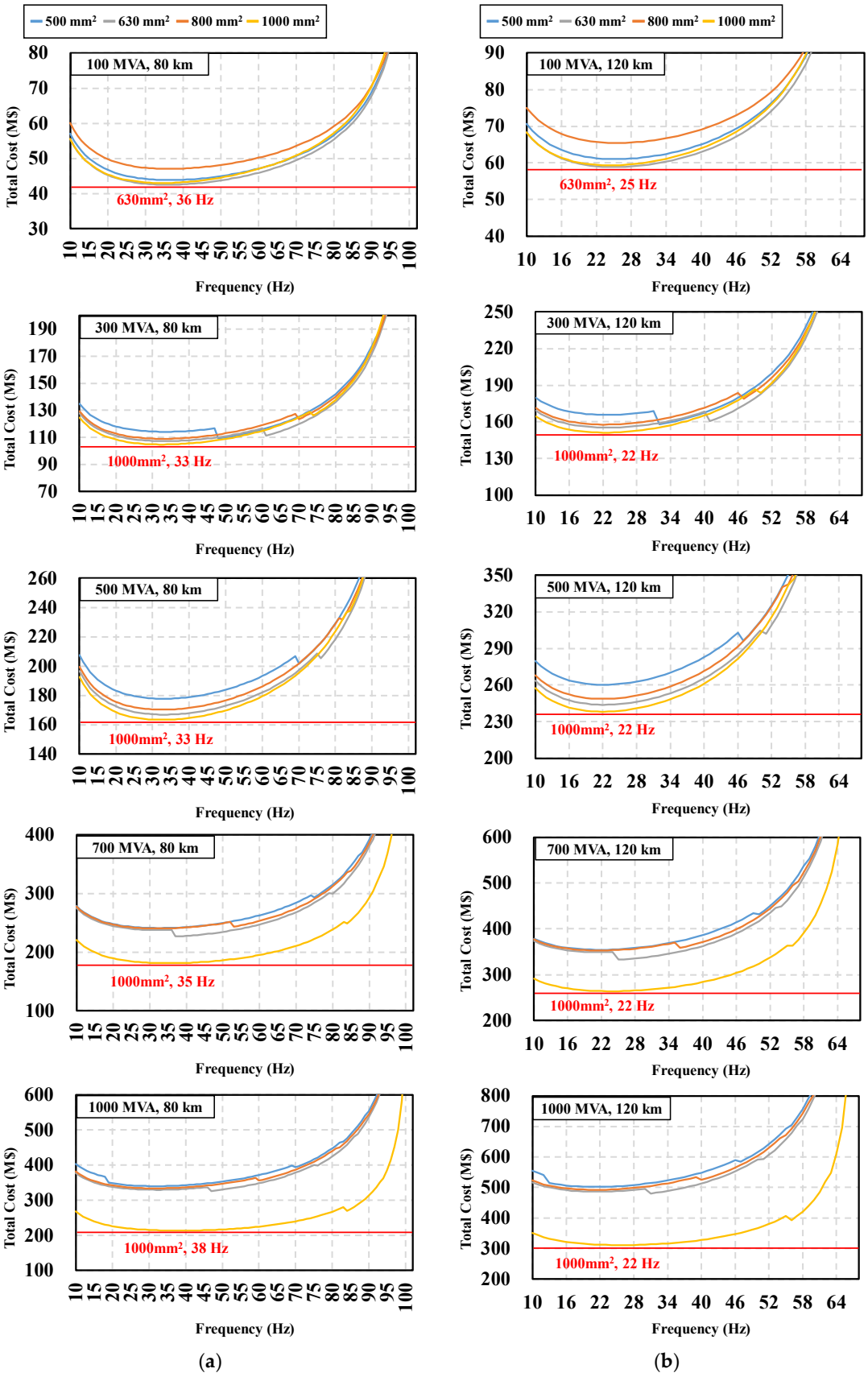

Figure 12. Total cost versus operating frequency at 220 kV: (**a**) 80 km; (**b**) 120 km.

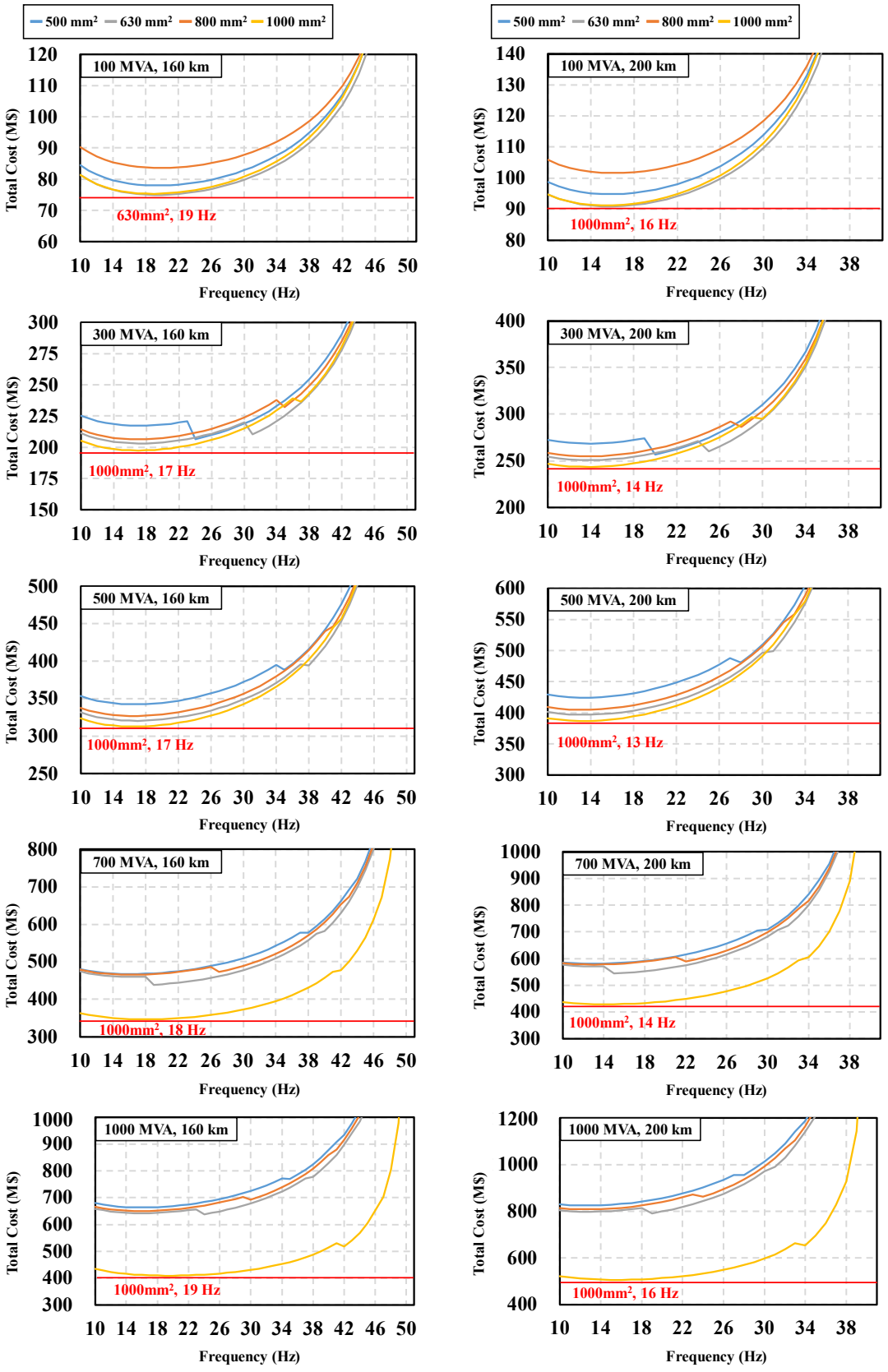

Figure 13. Total cost versus operating frequency at 220 kV: (**a**) 160 km; (**b**) 220 km.

3.2. Simulation Results

Figure 10a shows that as the transmission distance increases to 80 km, the optimal frequencies for capacities ranging from 100 to 500 MVA decrease to 42, 37, and 36 Hz. This decrease in optimal frequency with increasing capacity under the same cable specification of 630 mm^2 suggests that as the capacity increases, the amount of current, cables, and losses also increase, leading to a lower optimal frequency. For higher capacities such as 700 and 1000 MVA, the largest cable specification of 1000 mm^2 exhibits the most economical performance at 41 and 42 Hz. Similarly, as the capacity increases, the lower specifications necessitate an increase in the number of cables required for transmission, resulting in these outcomes.

Figure 11b represents the scenario with a transmission distance of 200 km under the same conditions. For capacities ranging from 100 to 500 MVA, using 630 mm^2 cables, the optimal frequencies decrease significantly to 18, 15, and 14 Hz compared to the 80 km scenario. This substantial decrease in optimal frequency with longer transmission distances can be interpreted as a consequence of cable costs dominating over factors such as transformer size, cost, and offshore platform installation. Table 5 summarizes the results of the optimal frequency simulation for a rated voltage of 132 kV.

Table 5. Results of optimal frequency simulation (132 kV).

Nominal Voltage (kV)	Transmission Length (km)	Wind Farm Capacity (MVA)	Optimal Frequency (Hz)	Cable Size (mm^2)	Total Cost (k$)
132	80	100	42	630	49,091
		300	37	630	131,666
		500	36	630	215,784
		700	41	1000	246,328
		1000	42	1000	299,683
	120	100	29	630	70,881
		300	25	630	192,922
		500	24	630	318,165
		700	27	1000	362,993
		1000	28	1000	442,090
	160	100	22	630	91,694
		300	19	630	253,964
		500	18	630	420,251
		700	21	1000	479,684
		1000	22	1000	584,314
	200	100	18	630	112,418
		300	15	630	314,848
		500	14	630	522,195
		700	17	1000	596,111
		1000	17	1000	725,881

The results shown in Figure 12a, with a rated voltage of 220 kV and a transmission distance of 80 km, indicate that the optimal frequencies decrease to 36, 33, and 33 Hz for capacities ranging from 100 to 500 MVA. This decrease in optimal frequency with increasing capacity can be interpreted similarly to the previous results; that is, as the capacity increases, the optimal frequency decreases to maintain the power transmission capacity. Furthermore, voltages greater than 132 kV result in high reactive power owing to the increase in capacity, leading to a low frequency.

As explained earlier, losses, reactive power, and the number of cables increase as capacity increases, necessitating a lower frequency. However, the frequency increases again

for capacities of 700 to 1000 MVA, which can be attributed to the capacity of the 1000 mm^2 cable. Because the rated capacity of the cable is large, while the number of cables remains similar, the costs of transformers and offshore platforms increase exponentially with capacity. Therefore, unless the transmission capacity significantly exceeds the rated capacity of the cable, it is interpreted that the optimal frequency increases as the capacity increases.

Figure 13b depicts the scenario with a transmission distance of 200 km, showing a decrease in the optimal frequency to 13–16 Hz as the transmission distance increases. Table 6 summarizes the results of the optimal frequency simulation for a rated voltage of 220 kV.

Table 6. Results of optimal frequency simulation (220 kV).

Nominal Voltage (kV)	Transmission Length (km)	Wind Farm Capacity (MVA)	Optimal Frequency (Hz)	Cable Size (mm^2)	Total Cost (k$)
220	80	100	36	630	42,532
		300	33	1000	104,686
		500	33	1000	163,302
		700	35	1000	181,004
		1000	38	1000	213,352
	120	100	25	630	58,847
		300	22	1000	151,197
		500	22	1000	238,158
		700	24	1000	263,837
		1000	26	1000	311,244
	160	100	19	630	74,958
		300	17	1000	197,453
		500	17	1000	312,743
		700	18	1000	346,303
		1000	19	1000	408,729
	200	100	16	630	90,943
		300	14	1000	243,593
		500	13	1000	387,090
		700	14	1000	428,586
		1000	16	1000	506,008

Tables 5 and 6 show that the total cost is lower for a rated voltage of 220 kV than for 132 kV. Furthermore, as the capacity increases, the difference in cost also increases, indicating that higher capacities are more advantageous with higher rated voltages. This occurs because the losses incurred in the cables outweigh the compensating effect for capacitive reactive power generated by higher voltages.

Similarly, as the transmission distance increases, the losses in the cables become significant, and thus, higher rated voltages become favorable. However, if the rated voltage is too high, it can lead to increased reactive power and a shorter power transmission distance for the cables, necessitating careful selection of the cables to consider these factors.

4. Conclusions

This study introduces a method to identify the economically optimal frequency for LFAC systems integrated with offshore wind farms. Key components of LFAC systems, such as transformers, offshore platforms, and subsea cables, exhibit frequency-dependent characteristics, affecting investment costs due to frequency variations. As a result, this study calculates the costs of LFAC components and evaluates the impact of frequency, capacity, and distance on total costs.

When frequency decreases, transformers require an increase in the number of windings and core area, necessitating greater amounts of copper and iron for manufacturing and resulting in higher investment costs. Consequently, there is an inverse relationship between frequency and costs, with the transformer costs at 10 Hz approximately nine times higher than those at 120 Hz. The weight of equipment installed on offshore platforms influences overall platform costs. Given that AC substations, including transformers, must be placed on the platform, a decrease in frequency leads to higher platform installation costs. Thus, there is an inverse correlation between frequency and costs, with platform costs at 10 Hz roughly three times higher than at 120 Hz. Subsea cable costs are determined by the quantity of cables needed for a given capacity and the need for reactive power compensation equipment. As the frequency decreases, the charging current decreases, which increases the transmission capacity and suppresses the reactive power generation. Hence, subsea cable costs are directly proportional to frequency.

The simulation results revealed that when distance remains constant, increasing capacity favors lower frequencies due to an increase in reactive power, losses, and the number of cables required. However, upon reaching a critical capacity, there is a tendency to shift towards higher frequencies. This shift is attributed to the advantages of utilizing cables with larger cross-sectional areas, which decrease losses and reduce the number of cables needed, thus offsetting the installation costs.

A comparison of 80 km and 200 km distances at 132 kV and 500 MVA showed optimal frequencies of 36 Hz and 14 Hz, respectively, with the optimal frequency for the 200 km distance being notably lower. This is explained by the considerable increase in cable costs compared to transformer and offshore platform costs as distance increases. Furthermore, a comparison of rated voltage levels demonstrated that using 220 kV resulted in lower total costs compared to 132 kV. This outcome is attributed to the greater impact of loss reduction in cables compared to the benefits of reactive power compensation from the increase in rated voltage.

This paper's analysis does not account for the efficiency of transformers and wind turbines, the operational conditions and efficiency of power conversion devices, the voltage stability of LFAC systems, or thermal limits. Operation at non-standard frequencies may affect equipment designed for standard frequencies, suggesting that future research should focus on selecting an economical frequency within stable conditions while taking existing equipment into account.

Author Contributions: Conceptualization, T.P. and B.A.; methodology, B.A.; formal analysis, T.K. and J.C.; simulation, B.A and J.C.; writing—original draft preparation, B.A.; writing—review and editing, T.P. and B.A. All authors have read and agreed to the published version of the manuscript.

Funding: This work was supported by the National Research Foundation of Korea (NRF) grant funded by the Korean government (MSIT) (No. NRF-2022R1A2C1013445). This research was supported by Korea Electric Power Corporation (Grant number: R22XO02-20).

Data Availability Statement: The original contributions presented in the study are included in the article, further inquiries can be directed to the corresponding author.

Conflicts of Interest: The authors declare no conflict of interest.

References

1. Wiser, R.H.; Bolinger, M. *2017 Wind Technologies Market Report*; U. S. Department of Energy: Washington, DC, USA, 2018.
2. UK Offshore Wind Capacity Factors of Energy Numbers. Available online: https://energynumbers.info/uk-offshore-wind-capacity-factors (accessed on 19 June 2022).
3. Bogdanović, M.; Ivošević, Š. Winds of Change: A Study on the Resource Viability of Offshore Wind Energy in Montenegro. *Energies* **2024**, *17*, 1852. [CrossRef]
4. Offshore Wind in Europe of Wind Europe. Available online: https://windeurope.org/wp-content/uploads/files/about-wind/statistics/WindEurope-Annual-Offshore-Statistics-2019.pdf (accessed on 21 February 2020).
5. IRENA—International Renewable Energy Agency. *World Energy Transition 1.5° Pathway*; IRENA: Masdar City, United Arab Emirates, 2022.

6. Conlon, T.; Waite, M.; Modi, V. Assessing new transmission and energy storage in achieving increasing renewable generation targets in a regional grid. *Appl. Energy* **2019**, *250*, 1085–1098. [CrossRef]
7. Liserre, M.; Cardenas, R.; Molinas, M.; Rodriguez, J. Overview of multi-MW wind turbines and wind parks. *IEEE Trans. Ind. Electron.* **2011**, *58*, 1081–1095. [CrossRef]
8. Bresesti, P.; Kling, W.L.; Hendriks, R.L.; Vailati, R. HVDC connection of offshore wind farms to the transmission system. *IEEE Trans Energy Convers.* **2007**, *22*, 37–43. [CrossRef]
9. Ryndzionek, R.; Sienkiewicz, Ł. Evolution of the HVDC link connecting offshore wind farms to onshore power systems. *Energies* **2020**, *13*, 1914. [CrossRef]
10. Bahrman, M.P.; Johnson, B.K. The ABCs of HVDC transmission technologies. *IEEE Power Energy Mag.* **2007**, *5*, 32–44. [CrossRef]
11. Van Hertem, D.; Ghandhari, M. Multi-terminal VSC HVDC for the European supergrid: Obstacles. *Renew. Sustain. Energy Rev.* **2010**, *14*, 3156–3163. [CrossRef]
12. Elliott, D.; Bell, K.R.; Finney, S.J. A comparison of AC and HVDC options for the connection of offshore wind generation in Great Britain. *IEEE Trans. Power Deliv.* **2015**, *31*, 798–809. [CrossRef]
13. Arrillaga, J.; Liu, Y.H.; Watson, N.R. *Flexible Power Transmission: The HVDC Options*; John Wiley & Sons: Hoboken, NJ, USA, 2007.
14. ALSTOM (Firm). *HVDC: Connecting to the Future*; ICON Group International: Las Vegas, NV, USA, 2010.
15. Hornsea Project One-Project Overview: Presentation for Ofgem OFTO. Available online: https://www.ofgem.gov.uk/sites/default/files/docs/2018/10/hornsea_one_project_presentation.pdf (accessed on 9 October 2018).
16. SSE. The Project at a Glance. Available online: https://doggerbank.com/downloads/3-Dogger-Bank-at-a-glance.pdf (accessed on 16 January 2019).
17. Chaithanya, S.; Reddy, V.B.; Kiranmayi, R. A state of art review on offshore wind power transmission using low frequency AC system. *Int. J. Renew. Energy Res.* **2018**, *8*, 141–149.
18. Liu, S.; Wang, X.; Ning, L.; Wang, B.; Lu, M.; Shao, C. Integrating offshore wind power via fractional frequency transmission system. *IEEE Trans. Power Del.* **2015**, *32*, 1253–1261. [CrossRef]
19. Li, J.; Zhang, X. Small signal stability of fractional frequency transmission system with offshore wind farms. *IEEE Trans. Sustain. Energy* **2016**, *7*, 1538–1546. [CrossRef]
20. Wang, X.; Wang, X. Feasibility study of fractional frequency transmission system. *IEEE Trans. Power Syst.* **1996**, *11*, 962–967. [CrossRef] [PubMed]
21. Fischer, W.; Braun, R.; Erlich, I. Low frequency high voltage offshore grid for transmission of renewable power. In Proceedings of the 2012 3rd IEEE PES ISGT Europe, Berlin, Germany, 14–17 October 2012; pp. 1–6.
22. Olsen, E.; Axelsson, U.; Canelhas, A.; Karamitsos, S. Low frequency AC transmission on large scale offshore wind power plants. In Proceedings of the 13th Wind Integration Workshop: International Workshop on Large-Scale Integration of Wind Power into Power Systems as well as on Transmission Networks for Offshore Wind Power Plants, Helsinki, Finland, 8–11 October 2014.
23. Hytten, L. Power Frequency Optimisation for Offshore Wind Farms. 2015. Available online: https://www.sintef.no/globalassets/project/eera-deepwind-2015/presentations/a/a2_hytten_dnvgl.pdf (accessed on 4 February 2015).
24. Xiang, X.; Fan, S.; Gu, Y.; Ming, W.; Wu, J.; Li, W.; He, X.; Green, T.C. Comparison of cost-effective distances for LFAC with HVAC and HVDC in their connections for offshore and remote onshore wind energy. *CSEE J. Power Energy Syst.* **2021**, *7*, 954–975.
25. Stehly, T.; Duffy, P. *2021 Cost of Wind Energy Review [Slides]*; U.S. Department of Energy: Washington, DC, USA, 2023.
26. Laury, J.; Abrahamsson, L.; Bollen, M.H. A rotary frequency converter model for electromechanical transient studies of 1623 Hz railway systems. *Int. J. Electr. Power Energy Syst.* **2019**, *106*, 467–476. [CrossRef]
27. Steimel, A. Power-electronic grid supply of AC railway systems. In Proceedings of the 2012 13th International Conference on Optimization of Electrical and Electronic Equipment (OPTIM), Chengdu, China, 14–17 September 2012; pp. 16–25.
28. Flourentzou, N.; Agelidis, V.G.; Demetriades, G.D. VSC-based HVDC power transmission systems: An overview. *IEEE Trans. Power Electron.* **2009**, *24*, 592–602. [CrossRef]
29. Ruddy, J.; Meere, R.; O'Donnell, T. Low Frequency AC transmission as an alternative to VSC-HVDC for grid interconnection of offshore wind. In Proceedings of the 2015 IEEE Eindhoven PowerTech, Eindhoven, The Netherlands, 29 June–2 July 2015; pp. 1–6.
30. Carrasco, M.; Mancilla-David, F.; Venkataramanan, G.; Reed, J. Low frequency HVAC transmission to increase power transfer capacity. In Proceedings of the 2014 IEEE PES T&D Conference and Exposition, Chicago, IL, USA, 4–7 May 2014; pp. 1–5.
31. Miura, Y.; Mizutani, T.; Ito, M.; Ise, T. Modular multilevel matrix converter for low frequency AC transmission. In Proceedings of the 2013 IEEE 10th International Conference on PEDS, Kitakyushu, Japan, 22–25 April 2013; pp. 1079–1084.
32. Zhang, Z.; Jin, Y.; Xu, Z. Modeling and control of modular multilevel matrix converter for low-frequency AC transmission. *Energies* **2023**, *16*, 3474. [CrossRef]
33. Domínguez-García, J.L.; Rogers, D.J.; Ugalde-Loo, C.E.; Liang, J.; Gomis-Bellmunt, O. Effect of non-standard operating frequencies on the economic cost of offshore AC networks. *Renew. Energy* **2012**, *44*, 267–280. [CrossRef]
34. Dicorato, M.; Forte, G.; Pisani, M.; Trovato, M. Guidelines for assessment of investment cost for offshore wind generation. *Renew. Energy* **2011**, *36*, 2043–2051. [CrossRef]
35. Olivares-Galván, J.C.; De León, F.; Georgilakis, P.S.; Escarela-Perez, R. Selection of copper against aluminium windings for distribution transformers. *IET Electr. Power Appl.* **2010**, *4*, 474–485. [CrossRef]
36. Kreider, M.; Oteri, F.; Robertson, A.; Constant, C.; Gill, E. *Offshore Wind Energy: Technology below the Water*; National Renewable Energy Laboratory (NREL): Golden, CO, USA, 2022.

37. DNV Danish Energy Agency. Cost and Performance Data for Offshore Hydrogen Production. Available online: https://ens.dk/sites/ens.dk/files/Energioer/cost_performance_data_offshore_hydrogen_production.pdf (accessed on 8 March 2023).
38. Nielsen, P. *Offshore Wind Energy Projects: Altener Project*, *Feasibility Study Guidelines*; SeaWind: Amsterdam, The Netherlands, 2003.
39. Ngo, T.; Lwin, M.; Santoso, S. Steady-state analysis and performance of low frequency AC transmission lines. *IEEE Trans. Power Syst.* **2015**, *31*, 3873–3880. [CrossRef]

Disclaimer/Publisher's Note: The statements, opinions and data contained in all publications are solely those of the individual author(s) and contributor(s) and not of MDPI and/or the editor(s). MDPI and/or the editor(s) disclaim responsibility for any injury to people or property resulting from any ideas, methods, instructions or products referred to in the content.